THE JOURNAL OF PHYSICAL CHEMISTRY B

Article

pubs.acs.org/JPCB

Optical Measures of Thermally Induced Chain Ordering and Oxidative Damage in Polythiophene Films

C. Carach and M. J. Gordon*

Department of Chemical Engineering, University of California Santa Barbara, Santa Barbara, California 93106-5080, United States

ABSTRACT: Thermally induced chain ordering (aggregation) and oxidative damage in neat poly(3-hexylthiophene) (P3HT) films were assessed using multiple optical metrics (low-temperature photoluminescence (LT-PL), Raman, absorbance, and IR spectroscopies) and NMR through quantitative analysis of exciton/chromophore bandwidths, emission, vibronic line shapes, and changes in film chemistry. Polymer morphology is discussed in light of how absorbance and PL provide complementary information about physically and chemically related changes in conjugation due to chain alignment (kinking and torsion), π-stacking, crystallite domain growth, and photo-oxidation. LT-PL is shown to be sensitive to oxidation phenomena, while absorbance and Raman are not; in contrast, aggregation can be most easily evaluated via absorbance using a Franck−Condon-like model of vibronic excitation. IR and NMR reveal how hexyl side chains and thiophene units are attacked during annealing in O_2. We also demonstrate that competition exists between the "disordering" effect of photodegradation and the physical "ordering" effect of aggregation, each of which dominates under different processing conditions. Ultimately, it is shown that various optical metrics of film disorder must be considered collectively to understand how processing affects film morphology.

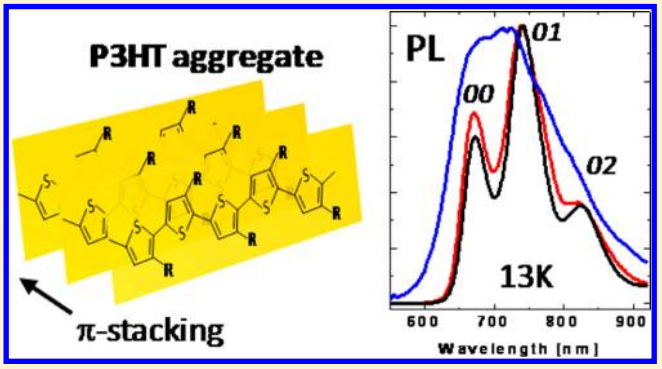

INTRODUCTION

Photovoltaic cells made from conjugated polymer−fullerene blends have attracted much interest due to their potential to provide electrical energy at low processing costs. These so-called "bulk heterojunction" (BHJ) solar cells produce current via light absorption in the polymer, followed by electron transfer to the fullerene acceptor at a molecular junction. Chemical tailoring of polymer properties (e.g., lower bandgap and higher mobility) and empirical tuning of polymer−fullerene morphology with processing has resulted in power conversion efficiencies above 8%.[1]

The morphology of the polymer−fullerene blend is commonly optimized via thermal annealing to transform the disordered, molecularly mixed structure into a more ordered, phase-separated morphology that enhances charge transport. In the case of the most widely studied BHJ blend, poly(3-hexylthiophene):[6,6]-phenyl-C_{61}-butyric acid methyl ester (P3HT:PCBM), annealing dynamics involve the growth of crystalline P3HT domains and the diffusion of PCBM through amorphous P3HT to form PCBM agglomerates.[2] Efforts to understand this complex morphology have spanned the entire realm of materials characterization techniques, from the most complex (e.g., synchrotron X-ray scattering,[2] tip-enhanced Raman spectroscopy,[3] and transient absorption[4]), to the more common (e.g., basic I−V testing[5]). Recent studies employing X-ray scattering show that the initial P3HT:PCBM BHJ morphology is composed of three phases: P3HT crystallites, PCBM agglomerates, and a "solution" of molecularly dispersed PCBM and amorphous P3HT.[2] Thermal annealing induces the diffusion and growth of PCBM agglomerates as well as the growth of P3HT crystallites[2,6] along the aliphatic (side chain) "*a*"-axis only; interestingly, the domain size in the π-stacking ("*b*") axis was not observed to change. This finding is rather curious because it is π-orbital coupling along the *b*-axis, in addition to transport along the polymer chain axis, that makes conjugated polymers useful in photovoltaic devices—that is, excitons (and free polarons) can travel between π-stacked polymer chains and the enhanced conjugation length in the π-axis leads to a favorable red shift[7] in absorbance.

Optical experiments on P3HT show that absorbance and emission line shapes are affected by π-stacking. This data has been interpreted by modeling the electronic structure of π-stacked P3HT as cofacially stacked, "H-aggregated" dye molecules[8] (we will take "π-stacked" to be synonymous with "aggregated" or "H-aggregated" throughout). In fact, absorbance and PL can provide a wealth of information about the extent and uniformity of π-stacking as well as the intrachain conjugation length in P3HT. For instance, fitting the absorbance spectrum of P3HT to the H-aggregate model has shown that conjugation length increases with the boiling point of the solvent from which the film was cast[9] (notwithstanding the fact that the films were also annealed, which can affect aggregation also). P3HT is also very sensitive to oxidative degredation;[10] as such, "physical" aggregation phenomena (e.g.,

Received: July 27, 2012
Revised: January 23, 2013
Published: January 24, 2013

   dx.doi.org/10.1021/jp307474u | *J. Phys. Chem. B* 2013, 117, 1950−1957

chain rearrangements, aggregate growth, etc.) must be considered in light of the fact that chemical attack of the polymer can also lead to chromophore and conjugation loss, which may otherwise be interpreted as physical disorder. We specifically address these convoluted issues in this work using complementary optical techniques (low-temperature PL, absorbance, Raman, and IR) to study how the electronic structure of P3HT is affected by *physical* (aggregate growth, planarization, etc.) and *chemical* (oxidative damage) processes as a function of thermal annealing (low- and high-T) and background atmosphere (inert, O_2, etc.). Overall, it is shown that multiple optical metrics should be used to assess competition between the "ordering" effect of polymer chain rearrangement during annealing and the apparent "disordering" effect of photo-oxidation for films processed under different oxygen exposure conditions. In particular, we show that (1) oxidative damage to P3HT can be witnessed easily via low-temperature PL, whereas Raman and absorbance are rather uninformative; (2) PL line-shape analysis and quenching must be considered collectively to assess polymer disorder; and (3) changes in polymer "ordering", which are thought to be due to physical effects, can be influenced considerably (or may be largely controlled) by chemical effects instead. This work also demonstrates that various optical metrics of film disorder should be viewed together to understand how processing affects film morphology and electronic structure; ultimately, reconciliation of these simple optical metrics could provide important clues and feedback to optimize device performance.

EXPERIMENTAL METHODS

Regioregular P3HT (M_W = 52 kDa, PDI = 2.2, Rieke 4002-EE, 91% head−tail-head−tail linkages as measured by ^{1}H NMR) was dissolved in chloroform (10 mg/mL) and spin-cast on ITO-coated glass slides to form thin films (~80 nm). P3HT films were annealed in a glovebox (<200 ppm O_2) or closed container on a calibrated hot plate in flowing Ar or O_2 (~500 sccm) in the dark, or under 365 nm illumination (~350 μW/cm^2). Absorbance data were taken using a home-built, double beam spectrometer (0.5 m Ebert monochromator with Hamamatsu R928 PMT). PL and Raman spectra were obtained with 457.9 or 514.5 nm pumping (Ar^+, ~2 mW, 300 μm spot, random polarization); light from the sample was collected with a 0.42NA long working distance objective and fiber-coupled to a JobinYvon iHR320 monochromator with cooled CCD detector. Samples were cooled to 13 K in a custom-built, closed-cycle helium refrigerator. IR spectra (500 averages/scan) were measured with a Bruker Equinox 55 FTIR with LN_2-cooled HgCdTe detector using P3HT samples spun on undoped Si. Liquid-phase ^{1}H NMR (Bruker 500 MHz) was acquired by dissolving the P3HT starting material or films spun on ITO in $CDCl_3$ with sonication. Summary data presented in Figure 7 (e.g., absorbance and PL metrics) represent an average of at least four measurement points on each film; thickness differences across films resulted in optical density variations <5%.

RESULTS AND DISCUSSION

I. General Trends in Absorbance and PL. Given the complex optical phenomena and diversity of results in the literature for P3HT, we start by briefly reviewing the current understanding of absorption and emission from conjugated polymer aggregates where vibronic (electron−phonon) coupling is important (Figure 1), as well as discuss common metrics used to assess chain organization. The broad

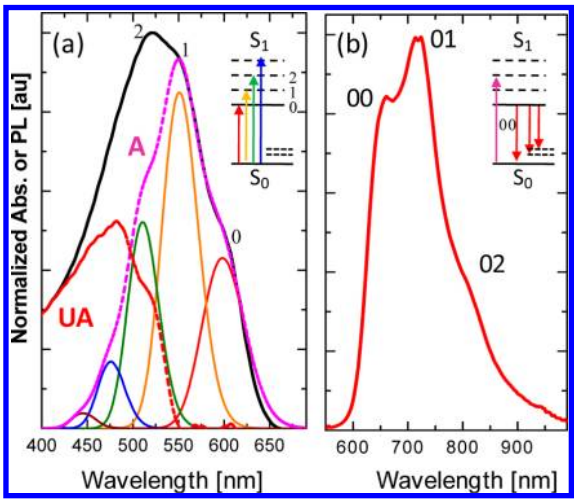

Figure 1. (a) Absorbance and (b) room temperature PL (514 nm pumping) spectra of as-cast ~80 nm thick P3HT film. Peak deconvolution in (a) shows absorption to different vibrational levels of the excited singlet state (0, 1, 2, ...), modeled using an H-aggregate-modified Franck−Condon fit. The "A" curve (dashed, purple) represents the total absorption associated with aggregated chains and the "UA" curve (dashed, red), representing unaggregated P3HT chains, was determined by subtracting the "A" curve from the experimental data (heavy, black). Panel (b) details PL emission from the excited singlet state to different vibrational levels of the ground electronic state, i.e., the 00, 01, and 02 emissions. Fine structure in the PL is associated with Stokes losses (~1450 cm^{-1}) due to strong vibronic coupling. Insets show the various electronic (solid lines) and vibrationally excited states (dashed lines) involved in absorption and emission.

absorbance feature of an as-cast P3HT film (Figure 1a) can be assigned to the collective $\pi-\pi^*$ ($S_0 \rightarrow S_1$) transition of the polymer chain, where the shoulders in the >500 nm region are indicative of vibronic coupling involving the vibrationally excited states v = 0, 1, 2 of S_1 (the excited π^* state, or exciton). Based on the pioneering theoretical work of Spano,[8] the absorbance spectrum can be thought of as a combination of (i) low-energy aggregated states ("A") that are a superposition of vibronic transitions involving Stokes losses from C=C bonds (i.e., simultaneous excitation of excitons and phonons), and (ii) a high-energy tail due to unaggregated P3HT chains ("UA"). The relative oscillator strengths of the vibronic transitions are perturbed from their single-molecule Franck−Condon (FC) form due to electronic coupling of P3HT chains along the π-axis. These absorption features can be modeled with a modified FC fit[8]

$$A = \sum_{m=0} \left(\frac{e^{-s} s^m}{m!} \right) \left(1 - \frac{We^{-s}}{2E_p} \left(\sum_{n \neq m} \frac{s^n}{n!(n-m)} \right) \right)^2 \exp\left[\frac{-(\hbar\omega - E_{0-0} - mE_p)^2}{2\sigma^2} \right] \quad (1)$$

where W is the exciton bandwidth, s is the Huang−Rhys factor,[9] E_p is the phonon (C=C) energy loss, E_{0-0} is the S_0-to-S_1 energy gap, σ is the Gaussian line width (i.e., E_{0-0} homogeneity), and ω is the light frequency. Since the exciton

dx.doi.org/10.1021/jp307474u | J. Phys. Chem. B 2013, 117, 1950−1957

bandwidth (W) is inversely proportional to the (intrachain) conjugation length,[10] fitting eq 1 to the measured absorbance spectrum can provide information about conjugation in the π-stacked aggregate (see Figure 1a).

We now move on to emission (Figure 1b); P3HT exhibits strong vibronic coupling in its photoluminescence (PL).[8c] For example, the 00, 01, and 02 shoulders in the PL correspond to transitions from the bottom of the $S_1(\pi^*,v=0)$ state to different vibrational levels of the electronic ground state S_0. These transitions are governed by selection rules peculiar to π-stacked polymer aggregates. The 00 transition is forbidden in a perfectly ordered H-aggregate (i.e., alternating dipole moments in adjacent chromophores cancel the overall transition moment associated with the 00 emission), and as such, the $R_{em} = I_{00}/I_{01}$ peak intensity ratio is a useful measure of π-stacking disorder.[8] However, due to scattering with lattice phonons and thermally activated emission from excitons above the bottom of the $S_1(v=0)$ band, i.e., line shape broadening,[11] the utility of R_{em} measurements at room temperature as a descriptor for organization is limited. For example, room temperature PL (RT-PL) from as-cast and Ar-annealed (160 °C, 30 min) P3HT films (Figure 2a) are virtually indistinguishable, and the O_2 annealed film appears slightly perturbed (increased broadening in the near-IR) from the as-cast case. However, very different observations are obtained when the PL is measured at low temperature (13 K, LT-PL), as depicted in Figure 2b. In this case, nonradiative losses and thermally activated hopping[11] are reduced, and emission proceeds preferentially (solely) from the bottom of S_1, resulting in a sharply peaked, slightly red-shifted spectrum for the as-cast and Ar-annealed films. Higher R_{em} and slightly increased broadening in the Ar-annealed case might suggest that H-like aggregation (π-stacking) has decreased with annealing. The O_2-annealed film has essentially no structure in either case, indicating destruction of the electronic structure characteristic to π-aggregated P3HT.

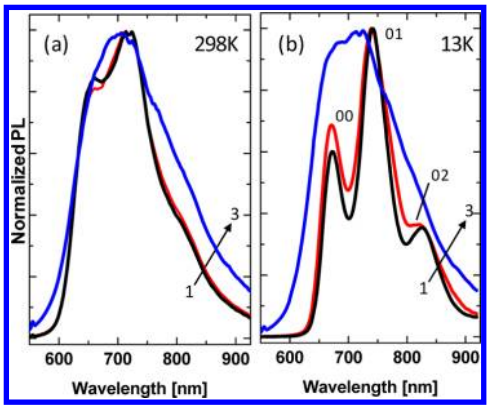

Figure 2. Evolution of (a) room temperature and (b) 13 K photoluminescence emission (514 nm pumping) of P3HT films annealed (160 °C/30 min) under different O_2 exposure conditions. Processing conditions were as follows: (1) as-cast film (no annealing); (2) Ar, dark; and (3) pure O_2, dark. The 00, 01, and 02 designations represent emission from the excited singlet state to the ground, first, and second vibrationally excited, ground electronic states, respectively.

II. Oxidation Effects. Oxidation is an important and arguably less studied topic related to OPV performance and lifetime.[12] Recent work suggests that oxygen radical attack of both the α-hydrogen and sulfur atoms of P3HT leads to the formation of alcohols, aldehydes, ketones, and sulfinate esters[13] which eventually destroy P3HT:PCBM solar cell devices. In the following sections, we show how IR spectroscopy and NMR provide clues about P3HT chemistry as a function of processing to provide a context to interpret absorbance and PL measures of polymer chain disorder related to physical (aggregation and packing) versus chemical (photo-oxidation) effects.

A. IR Spectroscopy. IR spectroscopy can be used to assess photo-oxidation of conjugated polymers and deduce the mechanism(s) of chain breakdown.[13] Here, we use IR to complement our LT-PL data (discussed later) with the overall intent to link changes in PL intensity and line shapes with chemical attack of the polymer. For example, Figure 3a,b shows how the aliphatic bonds (2800−3000 cm^{-1}) of the hexyl side chain of P3HT change with annealing time. Controlled photo-oxidation for 30 min at 100 °C under UV light and O_2 flow (red curve) leads to a slight reduction in absorbance, which does not appreciably change when the annealing time is extended to 120 min. Changes in other regions of the IR spectrum (e.g., C═C, C═O, thiophene C−H) were not observed. As such, we conclude that P3HT films processed under these relatively "mild" conditions may be subject to low levels of (oxidative) attack of the alkyl chains, but there is no evidence for destruction of the thiophene ring.

However, annealing under more extreme conditions (30 min, 160 °C, O_2) significantly reduces the aliphatic IR absorbance, as seen by the red curve in Figure 3b. Annealing for 140 min leads to further reduction of the aliphatic peaks; e.g., absorbance of the CH_2 in-plane vibration (1920 cm^{-1})[14] was reduced to ∼70% of its initial value. Longer annealing (270 min, not shown) did not result in further changes to the aliphatic region. Close examination of the fingerprint region (1300−1800 cm^{-1}, Figure 3c,d) shows that the thiophene ring is being attacked by oxygen; at 30 and 140 min, both the symmetric (shoulder at ∼1465 cm^{-1}) and asymmetric (peak at ∼1512 cm^{-1}) thiophene C−C stretches (denoted #) have decayed. Annealing also results in growth of (i) the carbonyl region (∼1620−1780 cm^{-1}),[13] particularly the peak at ∼1724 cm^{-1} (+), which signifies that oxygen is incorporated into P3HT; (ii) olefinic C═C species (∗ at 1612 and 1646 cm^{-1}); and (iii) peaks in the ∼1370 cm^{-1} region (× at 1355 and 1383 cm^{-1}) attributed to O−H bending modes.

Overall, IR spectroscopy results on P3HT indicate that (i) the thiophene ring is intact and a small fraction of alkyl chains may be damaged in films annealed under O_2/UV at 100 °C and (ii) annealing under O_2 at 160 °C leads to significant (oxidative) damage to both alkyl chains and the thiophene ring. It is important to note that the annealing conditions used for IR measurements, inasmuch as they provide a reference point for absorbance and PL measurements, were the most severe tested (e.g., 30 min/O_2/UV at 100 °C and 30 min/O_2 at 160 °C). It will be shown later that low-T PL is very sensitive to oxidative damage, both under severe annealing conditions as seen here (high temperature, high oxygen) as well as mild conditions (low temperature, inert environment) where changes in IR absorbance are extremely small or inconclusive.

B. NMR. Chemical attack of P3HT chains during film annealing in O_2 was investigated using ^1H NMR as shown in Figure 4 (see ref 15 for peak identifications). Several general trends occur upon annealing: (i) the aromatic "g" proton (7.0 ppm) on the thiophene ring associated with head−tail-head−tail monomer confirmation totally disappears, (ii) aliphatic protons on the hexyl side chain near the thiophene ring ("d−f")

dx.doi.org/10.1021/jp307474u | J. Phys. Chem. B 2013, 117, 1950−1957

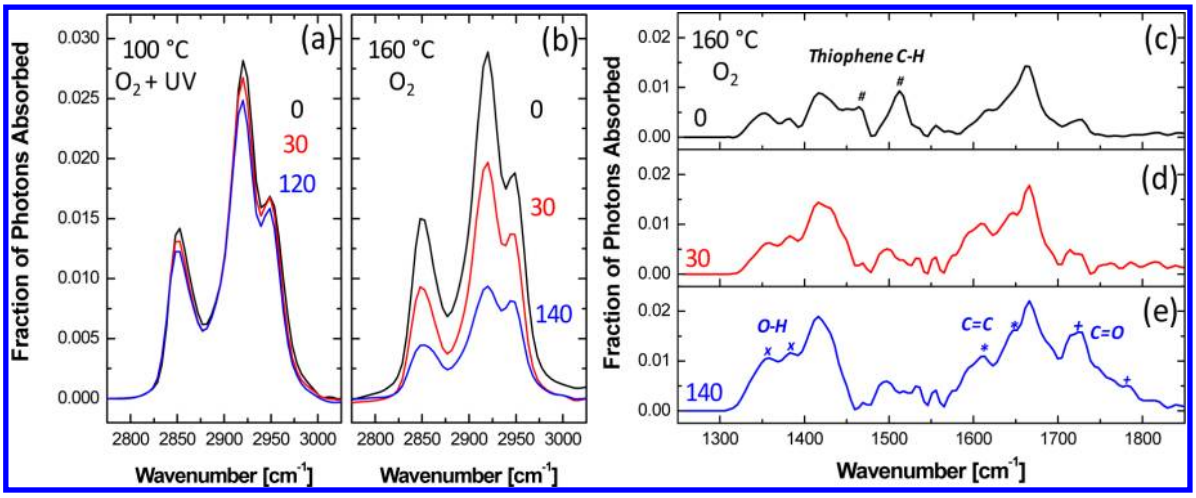

Figure 3. IR absorbance of P3HT films spun on undoped Si in the aliphatic (a,b) and fingerprint (c–e) regions as a function of annealing conditions in O_2. 0, 30, 120, and 140 refer to the annealing time in minutes at the condition listed. Thiophene C–H (#), O–H bending (×), C═C (∗), and C═O (+) vibrations are noted for reference in panels (c)–(e).

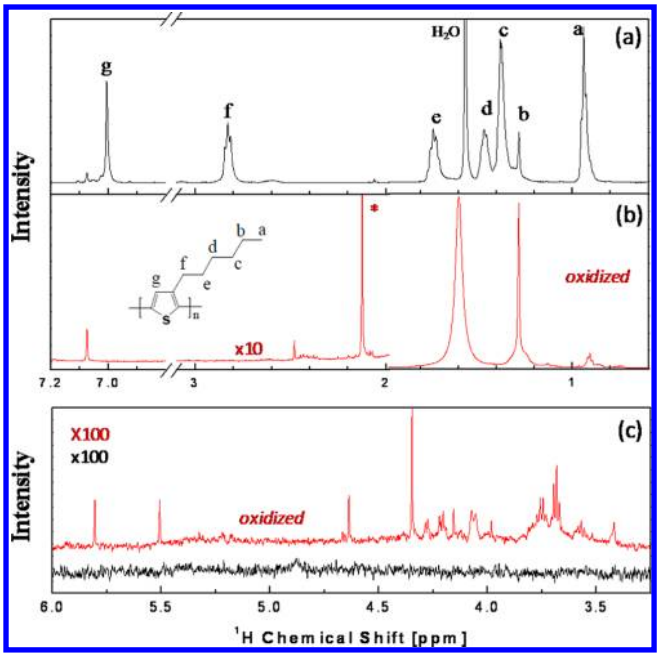

Figure 4. Liquid-phase ^{1}H NMR of (a) as-received P3HT and (b) annealed P3HT film (160 °C, pure O_2, 140 min) dissolved in $CDCl_3$. Peaks labeled a–g are associated with P3HT protons shown in the chemical structure inset. The peak at 1.56 ppm in panel (a) is due to water impurities in $CDCl_3$. The * peak in panel (b) at ∼2.1 ppm is generally associated with ketone or sulfenate species. (c) Zoom of the 3.5–6.0 ppm range. The multitude of peaks for the oxidized film can be generally assigned to different alcohol, sulfinate/sulfate, and olefinic protons formed by O_2 attack of the polymer. In general, annealing P3HT films in O_2 results in loss of the aromatic proton (g) and destruction of the hexyl side chain bonding near the thiophene ring (protons d, e, and f).

disappear, along with significant reduction in the $-CH_3$ proton "a" signal, and (iii) the oxidized film shows a multitude of new peaks in the 3.5–6.0 ppm range that can be generally assigned to different alcohol, sulfinate/sulfate, and olefinic protons (panel c).[15] These results clearly show that the polymer backbone and aliphatic side chain are severely attacked during O_2 annealing at 160 °C. We also note that the annealed film was very difficult to dissolve, another indicator that the aliphatic side chains were cleaved from the thiophene backbone and/or largely destroyed.

C. Raman Spectroscopy. As a matter of completeness, we should mention that the Raman shift of the P3HT ring-breathing mode (RBM) at ∼1450 cm^{-1} can be used as an indirect measure of conjugation length due to its symmetry with respect to the conjugation direction and change in nuclear coordinate from $S_0 \rightarrow S_1$.[16] Blue shifts (i.e., positive changes in cm^{-1}) of this Raman mode indicate reduced conjugation length; such changes have been used to measure the disordering effect of PCBM incorporation into P3HT films.[17a] In the present case with neat P3HT films, annealing at 160 °C for 30 min in O_2 caused a blue shift of ∼8 cm^{-1} in the RBM (see Figure 5). Closer examination also shows that the C═C

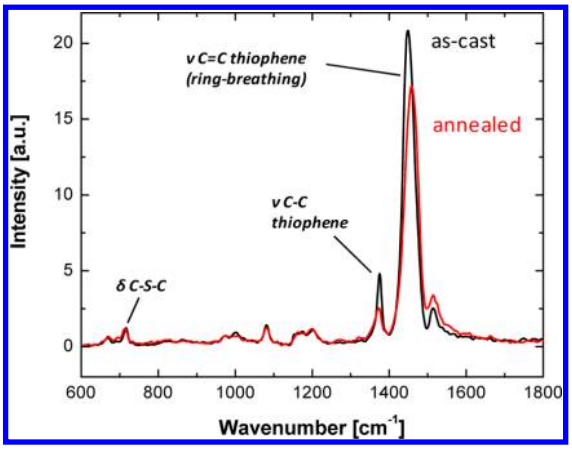

Figure 5. Raman spectra of as-cast (black) and annealed (30 min, 160 °C, O_2; red) P3HT films on ITO at 13 K. Annealing induces a blue shift of ∼8 cm^{-1} in the thiophene ring breathing mode (C═C, ∼1450 cm^{-1}) and a relative increase in the C–C mode at 1372 cm^{-1}.

(1450 cm^{-1}) to C–C (1372 cm^{-1}) ratio is higher (14.6 versus 10.3) for the annealed versus as-cast films; an increase in this ratio has been previously attributed to lower planarity of P3HT chains and an associated reduction in conjugation length.[7,17b] Because the RBM can be deconvoluted into a superposition of unaggregated (higher cm^{-1}) and aggregated (lower cm^{-1}) peaks,[7,17b] blue shifts can be attributed to an increase in

dx.doi.org/10.1021/jp307474u | J. Phys. Chem. B 2013, 117, 1950–1957

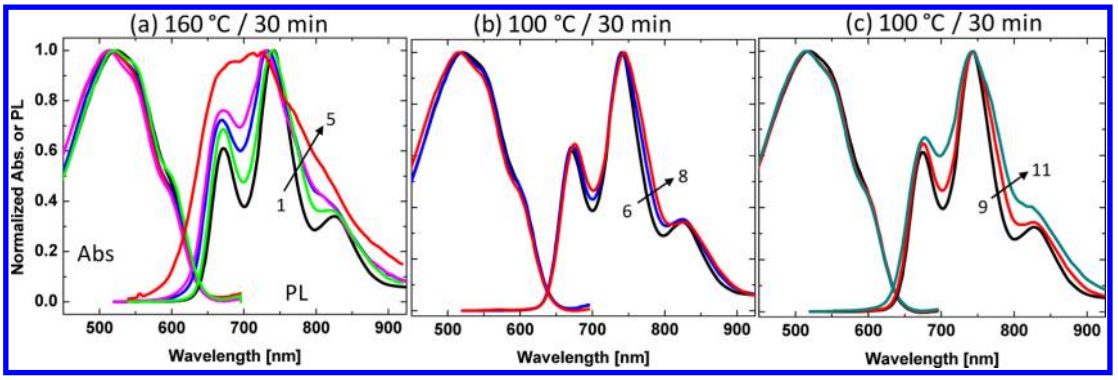

Figure 6. Normalized absorbance and low-temperature photoluminescence (13 K) spectroscopy (514 nm pumping) of P3HT films processed under different thermal annealing conditions. Curves are as follows: (1) as-cast; (2) glovebox (<200 ppm O_2), dark; (3) Ar, dark; (4) air, dark; (5) pure O_2, dark; (6) as-cast; (7) Ar, dark; (8) pure O_2, dark; (9) as-cast; (10) pure O_2, dark; (11) pure O_2 + 365 nm UV light.

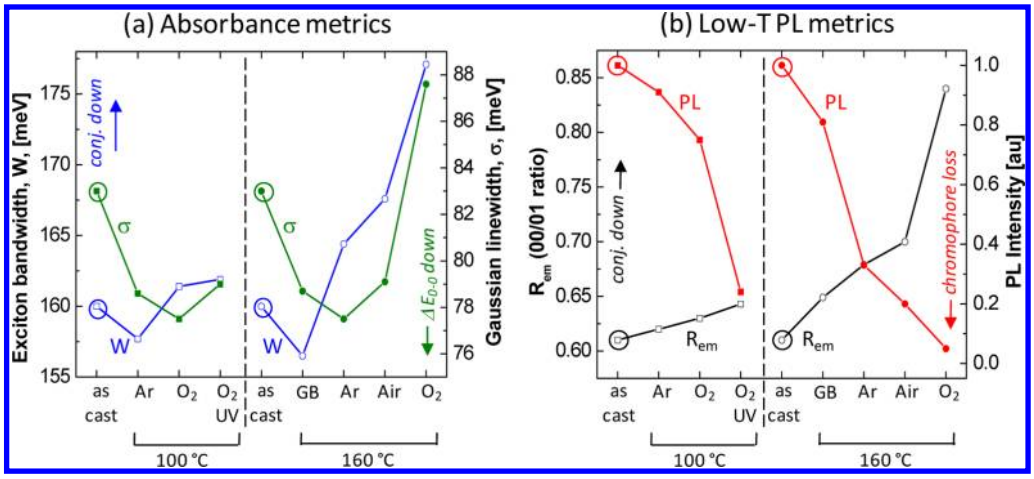

Figure 7. Summary of key optical metrics of P3HT chain "disorder" extracted from (a) absorbance and (b) low-*T* photoluminescence data in Figure 6 for various film processing conditions. Category labels represent films processed in argon + dark (Ar), O_2 + dark (O_2), glovebox with <200 ppm O_2 + dark (GB), air + dark (Air), or O_2 + 365 nm UV exposure (O_2/UV), respectively, at 100 or 160 °C for 30 min. In panel (a), the exciton bandwidth (W) and E_{0-0} homogeneity, as measured by the Gaussian line width σ, are represented on the left (open symbol) and right (closed symbol) axes, respectively. For panel (b), R_{em} is the 00/01 vibronic intensity ratio (left, open symbol) and the integrated PL emission (right, closed symbol), normalized to the as-cast film case. Data for the as-cast film are represented by circled points. Changes in conjugation length, loss of chromophores, and homogeneity of E_{0-0}, as implied from the data, are noted. See text for details on the various optical metrics.

unaggregated chains. However, it is improbable that annealing would lead to less aggregation and/or less planarity; as such, we ascribe the changes in the C═C (RBM) and C−C peaks as due to oxidation-induced conjugation reduction (i.e., *chemically induced* disorder) rather than changes in the *physical* alignment/packing of the P3HT chains (the interplay of physical versus chemical changes will be discussed in the next section). On a final note, we should mention that the RBM blue shift upon annealing could also be interpreted as aggregated chains being more susceptible to oxygen attack (i.e., less Raman intensity from aggregated chains compared to unaggregated). This seems unlikely if the oxidation reaction is limited by oxygen diffusion through the P3HT film, as aggregates have lower oxygen diffusion coefficients for poly(3-alkylthiophenes).[18] However, others have postulated that regions with higher conjugation length[19] (aggregated chains) may be more susceptible to oxygen attack because ionization potentials are lower than for unaggregated regions. The importance of and interplay between these two mechanisms is still under investigation.

The C−S−C vibration at ~700 cm^{-1} did not appear affected by O_2 annealing, though the line strength was very small. Changes in the RBM Raman shift for less severe annealing conditions were relatively small ($\leq$2 cm^{-1}) and do not show a monotonic progression with annealing severity. Furthermore, no changes in the C−C or C−S−C peaks were observed for less severe annealing conditions. As such, the Raman shift of the RBM, inasmuch as it can be a proxy for conjugation loss by way of reduced vibronic coupling, seems to be a less sensitive metric of oxidation-induced disorder compared to the low-T R_{em} ratio and PL intensity.

III. Physical versus Chemical Modification of Electronic Structure. Given the aforementioned backdrop, we now consider rigorous assessment of absorbance and low-*T*-PL metrics of P3HT films annealed in different environments and discuss general trends (see Figure 6). Changes in absorbance and PL can be associated with "electronic" disorder, which is due to both physical (i.e., changes in conjugation length due to chain kinking and torsion, aggregation phenomena related to π-stacking or crystallite domain growth, etc.) and/or chemical (e.g., oxidative defects) effects.

General trends in the absorbance and PL data with annealing can be summarized as follows: (i) absorbance changes are very small, especially for low annealing temperatures and (ii) low-*T* PL line shape (R_{em}), line broadening, and intensity appear more

dx.doi.org/10.1021/jp307474u | J. Phys. Chem. B 2013, 117, 1950−1957

sensitive to annealing temperature and O_2 background. Although absorbance changes are small, close inspection shows that (i) the low-energy vibronic shoulders (~550−625 nm) become better defined, and (ii) the absorbance envelope blue shifts. Since increased definition of absorbance shoulders is broadly associated with better polymer order but blue shifts are associated with disorder, interpretation of the absorbance spectrum based on inspection alone seems ambiguous. In fact, spectral deconvolution and parameter extraction using the H-aggregate model discussed earlier is necessary to make any conclusions from absorbance data. In contrast, LT-PL spectra display unambiguous changes upon superficial inspection; a clear trend of increasing R_{em} and line width with greater O_2 content and annealing temperature is readily apparent. These general tendencies are summarized more quantitatively using metrics related to conjugation length and π-stacking (i.e., exciton bandwidth, σ, R_{em}, and integrated PL intensity), as shown in Figure 7.

In general, absorbance metrics (W and σ, Figure 7a) indicate that mild annealing under low O_2 conditions (i.e., 100 °C in Ar or 160 °C in a glovebox with <200 ppm O_2) leads to a decrease in W (larger conjugation length) with a concomitant decrease in the Gaussian line width (σ), which indicates that the average chromophore energy gap (E_{0-0}) is more homogeneous. The former can be explained by (i) planarization of polymer chains or perhaps (ii) π-stacked aggregate growth in the b-axis at elevated temperature (which leads to better conjugation), and the latter can be attributed to more favorable chain alignment (greater uniformity of packing) in the b-axis. GI-XRD data mentioned in the Introduction eliminates explanation (ii) because domain growth in the b-axis has not been shown to occur under annealing. As such, absorbance data suggest that mild annealing of neat P3HT films results in H-aggregated P3HT domains composed of slightly straighter, more uniformly stacked polymer chains. We further note that W and σ say nothing about possible aggregate growth in the aliphatic a-axis. Alternatively, a rough measure of the total amount of aggregated P3HT can be obtained by taking the ratio of aggregated to unaggregated absorbance (A:UA in Figure 1) and adjusting for their respective oscillator strengths; such analysis has shown a slight increase in aggregated P3HT in neat films spun from high boiling point solvents.[9] Similar treatment of the data herein (chloroform solvent) gives an aggregate fraction of ~41% for all films (data omitted for brevity), with an insignificant (<2−3%) change upon annealing.

The remaining absorbance data generally show that W increases and σ decreases with the severity of the annealing process (e.g., higher T and/or higher O_2 result in larger changes; see Figure 7a) compared to the as-cast case. While the trend in σ still suggests more uniform packing, interpreting larger W as a reduction in conjugation on *physical* grounds seems implausible (i.e., P3HT chains should not "straighten out" during low-T annealing but "curl-up" during high-T annealing). The "reverse" trend in W with high-T annealing is more likely attributed to O_2-related defect generation that decreases π-orbital overlap between chains, rather than changes in chain linearity and planarity. This conclusion is discussed below in light of the PL and IR data, which indicate that chromophore loss is a more likely culprit.

The PL trends in Figures 6 and 7b show that the overall emission intensity decreases progressively with the severity of annealing in terms of temperature and oxygen environment, while R_{em} and vibronic peak line widths (webbing between the 00, 01, 02 peaks) steadily increase. Lower emission intensity is commonly attributed to two effects: (i) the population of aggregated chains has increased due to annealing (i.e., aggregates are less emissive[20] in some cases), and/or (ii) (oxidative) defects result in an effective loss of chromophores. Without complementary data, the dominant cause of the PL reduction remains ambiguous. The absorbance analysis discussed previously, as well as the aforementioned GI-XRD studies, would suggest that (i) does not occur (i.e., there is no crystal growth along the π-axis). The increase in R_{em} ratio and vibronic line width, which can only be quantitatively assessed at low temperature, indicates disordering of the polymer film with annealing under nearly all conditions. As before, a more physically disordered structure upon annealing is deemed as implausible. Moreover, the IR and NMR data shown in Figures 3 and 4 and discussed in section II conclusively show the presence of oxidized species after annealing (e.g., carbonyls, hydroxyls, sulfinates, and olefins). Therefore, the trend in R_{em} is only consistent with (ii); i.e., oxidative defects decrease the active chromophore population and reduce the effective π-stacking of polymer chains, which is (indirectly) observed as a loss of H-like aggregation (increasing R_{em}).

The fact that the more mildly annealed films exhibit changes in absorbance metrics (W and/or σ) that point to an increase in "order" on physical or structural grounds, coupled with changes in PL metrics that point to a decrease in "order" on chemical grounds (R_{em}), imply that (i) absorbance is more sensitive to "physical" ordering of P3HT, whereas LT-PL is more sensitive to chemical (oxidative) effects, and (ii) annealing P3HT films under similar conditions likely leads to simultaneous increases in both planarization/packing *and* oxidative damage. The increase in R_{em} upon annealing even in a controlled, low-oxygen environment illustrates how oxidation is extremely sensitive to annealing temperature (160 versus 100 °C). In fact, it has been shown that O_2 damage to conjugated polymers (PPVs) can take place "in an evacuated cryostat",[21] which we interpret as at least rough vacuum (<10 mTorr). Furthermore, LT-PL can even discern small changes that occur under milder annealing conditions at 100 °C (Figure 6b). Although changes in R_{em} are small for the Ar- and O_2-annealed films, the increased PL line widths ("webbing" of the vibronic peaks) give a clear image of the progression of disorder with annealing conditions. This study is extended one step further in Figure 6c, where the PL spectrum of an O_2-annealed film with UV illumination is added. The increased disorder is again seen through an increase in R_{em} and the broadening of the vibronic peaks, consistent with the accepted mechanisms of degradation hinging on UV-induced activation of oxygen radicals. It should be noted that the only change in the IR spectra of a similar film (30 min, 100 °C, O_2, UV, red curve, Figure 3a) is a very small reduction in the IR absorbance of the aliphatic C−H bonds, and the absorbance metrics (slightly smaller σ, slightly larger W, Figure 7a) are inconclusive due to their sensitivity to the simultaneously occurring physical aggregation. Therefore, out of the optical spectroscopy techniques employed (absorbance, IR, and PL), PL appears to be the most sensitive to oxidative disordering of P3HT.

The increased sensitivity of PL intensity to oxidation, as opposed to absorbance, can be explained by the propensity of excitons to migrate to highly electronegative chemical defects like carbonyls where they are quenched via electron transfer to the defect.[22,23] The PL yield is reduced not only by fewer photogenerated excitons (i.e., through reduced absorbance) but

dx.doi.org/10.1021/jp307474u | J. Phys. Chem. B 2013, 117, 1950−1957

also through oxidative defect-induced quenching. The qualitative changes in LT-PL spectra described here reinforce the idea of defect-induced disruption of conjugation (an effective increase in disorder) with increased annealing in O_2 that leads to an effective *decrease* in H-aggregation. This effect is clearly chemical in origin and competes with thermally driven physical reorganization processes which tend to *increase* linearity/planarity of polymer chains and aggregate growth in the aliphatic axis (only), where the former affects the quality of π-stacking (H-aggregation) but not the domain size (in the π-stacked direction).

CONCLUSIONS

Overall, we can say that multiple optical metrics should be used to evaluate processing-induced (dis)ordering in polythiophene films. In particular, we saw that absorbance (especially) and room temperature PL were relatively insensitive to annealing-induced ordering and oxidative attack of neat P3HT films cast from the same solvent. However, it was seen that low-T PL, where temperature-induced broadening and thermally activated emission from within the exciton band are minimized, was an effective and sensitive means to interrogate changes in π-conjugation due to mild annealing and/or oxidative defects. IR and NMR data from films annealed under severe conditions (30 min, 160 °C, O_2) show tell-tale signs of oxidative damage, i.e., attack/destruction of the aliphatic side chain and thiophene protons, creation of alcohol and sulfur−oxygen moieties, and the formation of carbonyl groups. Finally, this work shows that complementary (optical) metrics must be considered *collectively* to gain better insight into how film processing, through both physical *and* chemical phenomena, influences local morphology and electronic structure of conjugated polymer films.

AUTHOR INFORMATION

Notes

The authors declare no competing financial interest.

ACKNOWLEDGMENTS

This research work was supported by the MRSEC (seed) Program of the National Science Foundation under Award No. DMR-1121053 and the National Science Foundation CAREER program under Award No. CHE-0953441. The authors also thank L. C. Jones for NMR assistance and I. Riisness for helpful discussions.

REFERENCES

(1) He, Z.; Zhong, C.; Huang, X.; Wong, W.; Wu, H.; Chen, L.; Su, S.; Cao, Y. Simultaneous Enhancement of Open-Circuit Voltage, Short-Circuit Current Density, and Fill Factor in Polymer Solar Cells. *Adv. Mater.* **2011**, *23*, 4636−4643.

(2) Treat, N. D.; Brady, M. A.; Smith, G.; Toney, M. F.; Kramer, E. J.; Hawker, C. J.; Chabinyc, M. L. Interdiffusion of PCBM and P3HT Reveals Miscibility in a Photovoltaically Active Blend. *Adv. Energy Mater.* **2011**, *1*, 82−89.

(3) Wang, X.; Zhang, D.; Braun, K.; Egelhaaf, H.; Brabec, C. J.; Meixner, A. J. High-Resolution Spectroscopic Mapping of the Chemical Contrast from Nanometer Domains in P3HT:PCBM Organic Blend Films for Solar-Cell Applications. *Adv. Funct. Mater.* **2010**, *20*, 492−499.

(4) Grancini, G.; Polli, D.; Fazzi, D.; Cabanillas-Gonzalez, J.; Cerullo, G.; Lanzani, G. Transient Absorption Imaging of P3HT:PCBM Photovoltaic Blend: Evidence for Interfacial Charge Transfer State. *J. Phys. Chem. Lett.* **2011**, *2*, 1099−1105.

(5) Kim, Y.; Choulis, S. A.; Nelson, J.; Bradley, D. D. C.; Cook, S.; Durrant, J. R. Device Annealing Effect in Organic Solar Cells with Blends of Regioregular Poly(3-hexylthiophene) and Soluble Fullerene. *Appl. Phys. Lett.* **2005**, *86*, 063502.

(6) Lilliu, S.; Agostinelli, T.; Pires, E.; Hampton, M.; Nelson, J.; Macdonald, J. E. Dynamics of Crystallization and Disorder during Annealing of P3HT/PCBM Bulk Heterojunctions. *Macromolecules* **2011**, *44*, 2725−2734.

(7) Tsoi, W. C.; James, J. T.; Kim, J. S.; Nicholson, P. G.; Murphy, C. E.; Bradley, D. D. C.; Nelson, J.; Kim, J. The Nature of In-Plane Skeleton Raman Modes of P3HT and Their Correlation to the Degree of Molecular Order in P3HT:PCBM Blend Thin Films. *J. Am. Chem. Soc.* **2011**, *133*, 9834−9843.

(8) (a) Spano, F. C. Modeling Disorder in Polymer Aggregates: The Optical Spectroscopy of Regioregular Poly(3-hexylthiophene) Thin Films. *J. Chem. Phys.* **2005**, *122*, 234701. (b) Spano, F. C.; Clark, J.; Silva, C.; Friend, R. H. Determining Exciton Coherence from the Photoluminescence Spectral Line Shape in Poly(3-hexylthiophene) Thin Films. *J. Chem. Phys.* **2009**, *130*, 074904. (c) Spano, F. The Spectral Signatures of Frenkel Polarons in H- and J-Aggregates. *Acc. Chem. Res.* **2010**, *43*, 429−439.

(9) Clark, J.; Chang, J.; Spano, F. C.; Friend, R. H.; Silva, C. Determining Exciton Bandwidth and Film Microstructure in Polythiophene Films using Linear Absorption Spectroscopy. *Appl. Phys. Lett.* **2009**, *94*, 163306.

(10) (a) Cornil, J.; dos Santos, D. A.; Crispin, X.; Silbey, R.; Bredas, J. L. Influence of Interchain Interactions on the Absorption and Luminescence of Conjugated Oligomers and Polymers: A Quantum-Chemical Characterization. *J. Am. Chem. Soc.* **1998**, *120*, 1289−1299. (b) Manas, E. S.; Spano, F. C. Absorption and Spontaneous Emission in Aggregates of Conjugated Polymers. *J. Chem. Phys.* **1998**, *109*, 8087−8101. (c) Barford, W. Exciton Transfer Integrals Between Polymer Chains. *J. Chem. Phys.* **2007**, *126*, 134905.

(11) Mikhnenko, O. V.; Cordella, F.; Sieval, A. B.; Hummelen, J. C.; Blom, P. W. M.; Loi, M. A. Temperature Dependence of Exciton Diffusion in Conjugated Polymers. *J. Phys. Chem. B* **2008**, *112*, 11601−11604.

(12) Jorgensen, M.; Norrman, K.; Krebs, F. C. Stability/degradation of Polymer Solar Cells. *Sol. Energy Mater. Sol. Cells* **2008**, *92*, 686−714.

(13) Manceau, M.; Rivaton, A.; Gardette, J.; Guillerez, S.; Lemaitre, N. The Mechanism of Photo- and Thermooxidation of Poly(3-hexylthiophene) (P3HT) Reconsidered. *Polym. Degrad. Stab.* **2009**, *94*, 898−907.

(14) Abdou, M. S. A.; Holdcroft, S. Mechanisms of Photodegradation of Poly(3-alkylthiophenes) in Solution. *Macromolecules* **1995**, *26*, 2954−2962.

(15) (a) Barbarella, G.; Bongini, A.; Zambianchi, M. Regiochemistry and Conformation of Poly(3-hexylthiophene) via the Synthesis and the Spectroscopic Characterization of the Model Configurational Triads. *Macromolecules* **1994**, *27*, 3039−3045. (b) Chen, T.; Wu, X.; Reike, R. Regiocontrolled Synthesis of Poly(3-alkylthiophenes) Mediated by Reike Zinc: Their Characterization and Solid-State Properties. *J. Am. Chem. Soc.* **1995**, *117*, 233−244. (c) Mao, H.; Xu, B.; Holdcroft, S. Synthesis and Structure-Property Relationships of Regioregular Poly(3-hexylthiophene). *Macromolecules* **1993**, *26*, 1163−1169.

(16) Agosti, E.; Rivola, M.; Hernandez, V.; Del Zoppo, M.; Zerbi, G. Electronic and Dynamical Effects from the Unusual Features of the Raman Spectra of Oligo and Polythiophenes. *Synth. Met.* **1999**, *100*, 101−112.

(17) (a) Carach, C.; Riisness, I.; Gordon, M. J. Raman and Low Temperature Photoluminescence Spectroscopy of Polymer Disorder in Bulk Heterojunction Solar Cell Films. *Appl. Phys. Lett.* **2012**, *101*, 083302. (b) Gao, Y.; Grey, J. K. Resonance Chemical Imaging of Polythiophene/Fullerene Photovoltaic Thin Films: Mapping Morphology-Dependent Aggregated and Unaggregated C═C Species. *J. Am. Chem. Soc.* **2009**, *131*, 9654−9662.

(18) Luer, L.; Egelhaaf, H.-J.; Oelkrug, D.; Cerullo, G.; Lanzani, G.; Huis; n, B.-H.; de Leeuw, D. Oxygen-induced Quenching of

Photoexcited States in Polythiophene Films. *Org. Electron.* **2004**, *5*, 83−89.
(19) Abdou, M. S. A.; Orfino, F. P.; Son, Y.; Holdcroft, S. Interaction of Oxygen with Conjugated Polymers: Charge Transfer Complex Formation with Poly(3-alkylthiophenes). *J. Am. Chem. Soc.* **1997**, *119*, 4518−4524.
(20) Nguyen, T.-Q.; Martini, I. B.; Liu, J.; Schwartz, B. J. Controlling Interchain Interactions in Conjugated Polymers: The Effects of Chain Morphology on Exciton-Exciton Annihilation and Aggregation in MEH-PPV Films. *J. Phys. Chem. B* **2000**, *104*, 237−255.
(21) Klimov, V. I.; McBranch, D. W.; Barashkov, N. N.; Ferraris, J. P. Femtosecond Dynamics of Excitons in π-conjugated Oligomers: The Role of Intrachain Two-Exciton States in the Formation of Interchain Species. *Chem. Phys. Lett.* **1997**, *277*, 109−117.
(22) Chang, Y.; Su, W.; Wang, L. Influence of Photo-induced Degradation on the Optoelectronic Properties of Regioregular Poly(3-hexylthiophene). *Sol. Energy Mater. Sol. Cells* **2008**, *92*, 761−765.
(23) Yan, M.; Rothberg, L. J.; Papadimitrakopolos, F.; Galvin, M. E.; Miller, T. M. Defect Quenching of Conjugated Polymer Luminescence. *Phys. Rev. Lett.* **1994**, *73*, 744−747.